J. Biochem. 121, 477-486 (1997)

In Vitro Assembly of FAD, AMP, and the Two Subunits of Electron-Transferring Flavoprotein: An Important Role of AMP Related with the Conformational Change of the Apoprotein[1]

Kyosuke Sato, Yasuzo Nishina, and Kiyoshi Shiga

Department of Physiology, Kumamoto University School of Medicine, Honjo, Kumamoto, Kumamoto 860

Received for publication, September 9, 1996

Electron-transferring flavoprotein from pig kidney is composed of four non-covalently bound components: α and β subunits, flavin adenine dinucleotide (FAD), and adenosine monophosphate (AMP). This paper reveals the pathway of assembly of the electron-transferring flavoprotein. The holoprotein can be formed by two different pathways. (i) $\alpha+\beta \rightleftarrows (\alpha\text{-}\beta)^*$, $(\alpha\text{-}\beta)^*+\text{AMP} \rightleftarrows (\alpha\text{-}\beta\text{-AMP})^*$, $(\alpha\text{-}\beta\text{-AMP})^* \rightleftarrows \alpha\text{-}\beta\text{-AMP}$, $\alpha\text{-}\beta\text{-AMP}+\text{FAD} \rightleftarrows$ holoprotein. (ii) $\alpha+\beta \rightleftarrows \alpha\text{-}\beta$, $\alpha\text{-}\beta+\text{FAD} \rightleftarrows \alpha\text{-}\beta\text{-FAD}$, $\alpha\text{-}\beta\text{-FAD}+\text{AMP} \rightleftarrows$ holoprotein. Here the presence and absence of asterisks distinguish different conformations with the same composition. The monomeric forms of α and β showed no significant binding with FAD and AMP. AMP and FAD associated with different heterodimer forms which were formed as a result of weak binding between α and β. The binding of $\alpha+\beta+$AMP was much faster than that of $\alpha+\beta+$FAD because the rate of $\alpha+\beta \rightarrow (\alpha\text{-}\beta)^*$ was much faster than that of $\alpha+\beta \rightarrow \alpha\text{-}\beta$. The $\alpha\text{-}\beta$-AMP complex associated with FAD rapidly. As a result, the binding of FAD with the subunits is promoted by AMP. The $\alpha\text{-}\beta$-FAD complex associated with AMP much more slowly than the mixture of α and β. Thus the AMP binding with the subunits is inhibited by the preceding FAD binding.

Key words: AMP, assembly, conformation, electron-transferring flavoprotein, subunit.

Electron-transferring flavoprotein (ETF) is a mitochondrial protein (*1*) which serves as an electron acceptor of several mitochondrial dehydrogenases. Some of these dehydrogenases, such as short-, medium-, and long-chain acyl-CoA dehydrogenases (*2*), are included in the degradation system of fatty acids. Others, such as isovaleryl-CoA dehydrogenase (*3*) and 2-methyl butyryl-CoA dehydrogenase (*4*), are included in the catabolic system of amino acids. Thus, the electron abstraction from these dehydrogenases by ETF promotes energy production. In addition, the electrons accepted by ETF are transferred to the mitochondrial respiratory chain by way of ETF-CoQ oxidoreductase (*5*) and are used for ATP production at the end.

Mammalian ETF is composed of two nonidentical subunits and two small molecules, FAD and AMP (*6, 7*). These four components are bound tightly by non-covalent interactions. The subunit molecular weights were estimated (*8–11*) to be 33,000 for α subunit and 29,000 for β subunit. The crystal structure of ETF (*12, 13*) has not been published yet and the location of the binding sites of FAD and AMP are unknown.

It seems physiologically significant that ETF contains AMP because ETF works as a part of the ATP-synthesizing system. However, the function of AMP in the holoprotein form is presently unclear because AMP-deficient ETF has the same electron-transferring activity as the holoprotein (*6*). The role of AMP was suggested by the *in vitro* renaturation of ETF (*6*). In those experiments, the subunits unfolded by denaturant were diluted by buffer solution containing FAD and AMP. The subunit refolding and the assembly of the four components were initiated by the dilution. As shown by Fig. 6 in a previous paper (*6*), the binding between FAD and the subunits is made fast by AMP. This result indicated that the AMP plays a role in (i) the refolding steps of the subunits or (ii) the assembling process of the four components. In the preceding paper (*14*), we investigated the refolding and unfolding reactions of α and β subunits, and clarified that neither AMP nor FAD affects the subunit refolding.

The present study focuses on the later process, namely, assembly of the refolded subunits, FAD, and AMP. The clarified overall association pathway is summarized in Schemes 1 and 2. Here, $\alpha\text{-}\beta^A$ and $\alpha\text{-}\beta^F$ are two different forms of $\alpha\text{-}\beta$ complex and A* and A are two different forms of $\alpha\text{-}\beta$-AMP complex. In Scheme 1, AMP associates with the subunits before FAD does. In Scheme 2, the order is reversed. Based on these schemes, we discuss the role of AMP in the process of assembly. Further, we discuss the conformational change of the protein during the assembly. The protein conformation is closely related with its binding ability with FAD and AMP.

MATERIALS AND METHODS

Materials—ETF was purified from pig kidney by the method of Gorelick *et al.* (*9*) with some modifications (*15*).

[1] This work was supported in part by a Grant-in-Aid for Scientific Research from the Ministry of Education, Science, Sports and Culture of Japan.

Abbreviations: AMP, adenosine 5′-monophosphate; DTT, dithiothreitol; ETF, electron-transferring flavoprotein; FAD, flavin adenine dinucleotide.

Downloaded from http://jb.oxfordjournals.org/ at Changhua Christian Hospital on October 2, 2012

$$\alpha + \beta \underset{k_{-1}}{\overset{k_{+1}}{\rightleftharpoons}} \alpha\text{-}\beta^{A}$$
$$\alpha\text{-}\beta^{A} + \mathrm{AMP} \underset{k_{-2}}{\overset{k_{+2}}{\rightleftharpoons}} A^{*} \underset{k_{-3}}{\overset{k_{+3}}{\rightleftharpoons}} A$$
$$A + \mathrm{FAD} \underset{k_{-4}}{\overset{k_{+4}}{\rightleftharpoons}} \text{holoprotein} \qquad (1)$$

$$\alpha + \beta \underset{k_{-5}}{\overset{k_{+5}}{\rightleftharpoons}} \alpha\text{-}\beta^{F}$$
$$\alpha\text{-}\beta^{F} + \mathrm{FAD} \underset{k_{-6}}{\overset{k_{+6}}{\rightleftharpoons}} \alpha\text{-}\beta\text{-FAD}$$
$$\alpha\text{-}\beta\text{-FAD} + \mathrm{AMP} \underset{k_{-7}}{\overset{k_{+7}}{\rightleftharpoons}} \text{holoprotein} \qquad (2)$$

Schemes 1 and 2

The α and β subunits of ETF were separated in urea-denatured forms (*11*). FAD was purified as previously described (*6*). AMP was purchased from Sigma. Other chemicals were from Nacalai Tesque.

Molar Extinction Coefficients—Concentrations were determined spectrophotometrically using the following molar extinction coefficients: $\varepsilon_{275} = 15{,}600\ M^{-1}\cdot cm^{-1}$ for unfolded form of α (*11*), $\varepsilon_{280} = 8{,}300\ M^{-1}\cdot cm^{-1}$ for unfolded form of β (*11*), $\varepsilon_{450} = 11{,}300\ M^{-1}\cdot cm^{-1}$ for FAD (*16*), and $\varepsilon_{260} = 15{,}400\ M^{-1}\cdot cm^{-1}$ for AMP (*17*).

Buffer Conditions of the Reactions—Unless otherwise stated, all reactions were carried out in 50 mM potassium phosphate, pH 7.6, 5% v/v glycerol, 1 mM DTT, and 0.08 M urea at 25°C.

Preparation of Refolded Subunits—The contents of the stock solution of urea-denatured subunit was 100 μM α or β in 50 mM potassium phosphate buffer, pH 7.6, containing 4 M urea, 5% v/v glycerol, and 10 mM DTT. The refolded forms of α and β were prepared by diluting the urea-denatured subunits with buffer solution to give the final concentrations of 0.1-0.5 μM subunits and 0.08 M urea at 25°C. For the completion of the folding reaction, the diluted subunits were incubated for at least 20 min (*14*) before being used for experiments.

The concentration of the refolded subunit was checked by the flavin fluorescence increment after incubation with excess of the partner subunit, AMP, and FAD. The yield of the recoverable refolded subunit always exceeded 85% of the starting urea-denatured forms of subunits. The subunit concentration cited in this paper indicates the concentration of recoverable refolded subunit quantified in this way. The refolded subunits were stable below 0.5 μM: they lost only 2-4% of recoverability in 1 h.

Fluorometric Measurements—Flavin fluorescence was measured by 450-nm excitation and 490-nm detection. Protein fluorescence (tryptophan fluorescence) was measured by 300-nm excitation and 350-nm detection. The ordinate scales of the figures which display fluorescence time courses indicate the output value of the fluorimeter. The instruments were the same as those described previously (*14*).

Molar Extinction Coefficients of Subunits in the Presence of FAD or AMP—A gel filtration column (1.5×16 cm) filled with Sephadex G-25 superfine gel (Pharmacia) was fitted on an HPLC system and the temperature was maintained at 25°C. The buffer solution containing 0-80 μM AMP or 0-1 μM FAD was fed continuously at a rate of 1 ml/min. A 0.9-ml solution of 2 μM α or β containing AMP or FAD, the concentration of which was the same as that in the running buffer, was subjected to gel filtration. The elution was monitored by the absorbance and refractive index detectors connected in tandem.

The subunit eluted from the column should be in equilibrium with the AMP or FAD contained in the running buffer. If the subunit associates with the AMP or FAD, the peak height of the absorbance elution profile should be enlarged by the bound AMP or FAD. On the other hand, the perturbation of the refractive index elution profile by the binding of AMP or FAD should be very small, because the molecular weights of AMP and FAD are only 1-3% of those of the subunits.

The molar extinction coefficient, which is an indicator of the ligand binding, was determined as follows. The weight concentration (c_w) of the subunits at the peak is given by $c_w = RI/(dn/dc_w)$, where RI is the peak height of the refractive index and (dn/dc_w) is the specific refractive increment (n is refractive index). The molar concentration (c_m) of the subunits at the peak is given by $c_m = c_w/(M \times g/mol)$, where M is the molecular weight. Therefore, the molar extinction coefficient (ε) can be calculated by the equation,

$$\varepsilon = \frac{Abs}{c_m} = \frac{Abs}{RI} \times \left(\frac{dn}{dc_w}\right) \times M \times \frac{g}{mol},$$

where Abs is the peak height of the absorbance. We used the value of $dn/dc_w = 0.187\ ml\cdot g^{-1}$, which is common for simple proteins (*18*). The molecular weights determined by SDS-PAGE (*11*), 32,900 (α) and 28,600 (β), were used for the M value.

The amount of the subunit molecules eluted from the column was 70-80% of the loaded protein as judged by the peak area of the refractive index elution profile, and 70-75% as judged by the recovery to the holoprotein after incubation with the partner subunit, FAD, and AMP. This result confirms that the subunit eluted from the column is almost completely native.

Estimation of Apparent Molecular Weight—The apparent molecular weight was estimated by the method of Takagi *et al.* (*18, 19*), in which a light-scattering photometer and a refractometer were connected after a gel filtration column. Our system was described previously (*6*). The apparent molecular weight (M_{app}) can be obtained by

Downloaded from http://jb.oxfordjournals.org/ at Changhua Christian Hospital on October 2, 2012

the equation (*18, 19*),

$$M_{app} = \kappa \times \frac{LS}{RI}$$

where *LS* and *RI* are the peak heights of light-scattering and refractive index, respectively, and κ is the instrument constant.

Electrophoresis—Isoelectric focusing was carried out as described previously (*6*). Gel plates stained by Coomassie Brilliant Blue R-250 were scanned with an LKB 2202 UltroScan laser densitometer.

Calculations by Computer—Curve fitting (non-linear least-squares analysis) was performed by using the Gauss-Newton method. Time course of reaction was simulated by numerically solving differential equations by using the biquadratic Runge-Kutta method. The computer programs were originally written by us.

RESULTS

Reaction by Mixing All the Components of ETF—Figure 1 shows the time courses of the reactions of refolded α and β, FAD, and various concentrations of AMP. The enhancement of flavin fluorescence reflects the binding of FAD with α and β, because the FAD in the holoprotein is more fluorescent than free FAD (*9*) and the FAD in the α-β-FAD complex is as fluorescent as the FAD in the holoprotein (*6*). The result in Fig. 1 clearly shows that the binding of FAD with subunits is made fast by raising the AMP concentration. The concentrations of α and β also affected the reaction rate: the time required for the half completion was reduced by raising the concentrations of α and β. On the other hand, the concentration of FAD did not affect the time course in the range of 1-4 μM.

Interaction of Single Subunit with AMP and FAD—The possibility of complex formation between a single subunit (α or β) and a ligand (AMP or FAD) was examined by measuring the molar extinction coefficient (ε) of the subunit equilibrated with the solution containing AMP or FAD as described in "MATERIALS AND METHODS." In the absence of AMP and FAD, the extinction coefficients at 270 nm (ε_{270}) were estimated to be 14 (α) and 7.5 $mM^{-1} \cdot cm^{-1}$ (β). The ε_{270} values of the ligands, 10.3 (AMP) and 34 $mM^{-1} \cdot cm^{-1}$ (FAD), are both large enough for the binding to be detected. However, we detected no change of ε_{270} values of α and β in the presence of 0-80 μM AMP or 0-1 μM FAD, indicating that the single subunit binds neither AMP nor FAD in the absence of the partner subunit. This is consistent with our previous result (*11*): the protein and flavin fluorescence spectra were not altered by mixing single subunit, AMP, and FAD.

Interaction between α and β—Figure 2 shows the gel filtration of mixtures of α and β with different concentrations at injection. At low concentration (**1**), the peak of the elution profile (27.40 min) was located between the peaks of α (27.32 min) and β (27.45 min) chromatographed separately (data not shown). At higher concentrations (**2** and **3**), the peak of the subunit mixture appeared earlier, suggesting a weak association between α and β. This peak shift cannot be ascribed to interactions between the same subunit, because the peak positions of single subunits were not shifted by the concentration (data not shown).

The dissociation constant between α and β was estimated from the apparent molecular weight (M_{app}) measured by light-scattering (see "MATERIALS AND METHODS"). The M_{app} value of the subunit mixture at 1.5 μM was (59 $\pm$ 14)% of the M_{app} value of the holoprotein. This value corresponds to the degree of association of (18 $\pm$ 28)%: the subunits are almost in the monomer forms at 1.5 μM. Taking account of the error range, the dissociation constant between α and β can be estimated to be much higher than 1 μM. The dissociation constant could not be determined because of the aggregation of the subunits at high concentration (*11*).

Binding of α, β, and AMP—Figure 3A shows the time course of the tryptophan fluorescence of 0.1 μM α and β before and after the addition of 80 μM AMP. As shown in the inset of Fig. 3A, the relaxation curve fitted well with hyperbolic function of time (t).

$$Y(t) = \frac{Y_0 - Y_\infty}{k_{obs} t + 1} + Y_\infty \qquad (3)$$

$Y(t)$, Y_∞, and Y_0 are the fluorescence values at time t, infinite time, and zero time, respectively, and k_{obs} is the

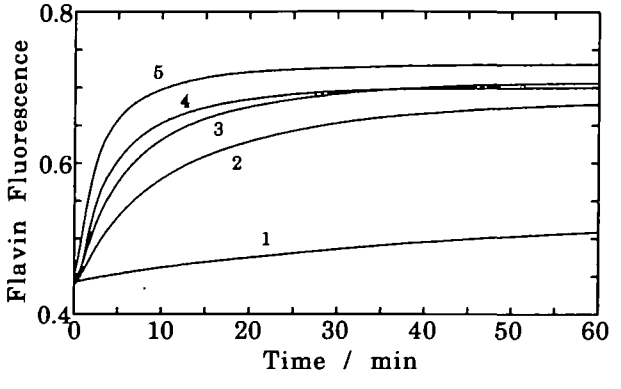

Fig. 1. **Effect of AMP on the reaction of α, β, FAD, and AMP.** Before the reaction, urea-denatured α and β were diluted with the buffer solution to give the final concentration of 0.2 μM in 2 ml and allowed to refold for 20 min. At zero time, small volume (4-14 μl) of FAD and AMP solution was added to the solution of the refolded subunits to give the final concentrations of 2 μM FAD, and 0 (1), 2.5 (2), 5 (3), 10 (4), or 20 μM (5) AMP.

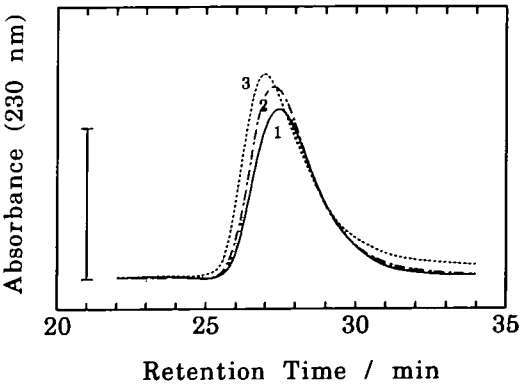

Fig. 2. **Molecular sieve chromatography of mixtures of α and β with different concentrations.** Mixtures of refolded α and β [0.0625 (1), 0.25 (2), or 1 μM (3)] in 1 ml of solution were loaded on a Superose 12 HR 10/30 column (Pharmacia) maintained at 25°C. The flow rate was 0.5 ml/min. The left-hand bar indicates the absorbance scale: 0.00625 (1), 0.025 (2), and 0.1 (3).

Downloaded from http://jb.oxfordjournals.org/ at Changhua Christian Hospital on October 2, 2012

observed rate constant.

In the previous sections, it was demonstrated that α and β weakly interact with each other and that a single subunit does not associate with AMP. These results lead to Scheme 4 as the mechanism of the binding of α, β, and AMP.

$$\alpha+\beta \underset{k_{-1}}{\overset{k_{+1}}{\rightleftharpoons}} \alpha\text{-}\beta^{A},\ \alpha\text{-}\beta^{A}+\mathrm{AMP} \xrightarrow{k_{+2}} \alpha\text{-}\beta\text{-AMP} \qquad (4)$$

In this scheme, AMP associates with a heterodimer form (α-β^{A}) which results from the weak binding between α and β. Using the steady state method with the assumptions of $[\alpha] \gg [\alpha\text{-}\beta^{A}]$ and $[\beta] \gg [\alpha\text{-}\beta^{A}]$, the reaction velocity ($v = \mathrm{d}[\alpha\text{-}\beta\text{-AMP}]/\mathrm{d}t$) is represented as

$$v=\frac{k_{+1}[\mathrm{AMP}][\alpha][\beta]}{k_{-1}/k_{+2}+[\mathrm{AMP}]}. \qquad (5)$$

Here, the brackets represent molar concentration. The time course should obey a hyperbolic function of time when the concentrations of α and β are identical to each other and the concentration of AMP is constant during the reaction. The observed rate constant should be

$$k_{\mathrm{obs}}=\frac{k_{+1}[\mathrm{AMP}]c_0}{k_{-1}/k_{+2}+[\mathrm{AMP}]}, \qquad (6)$$

where c_0 is the starting concentration of each subunit. This equation implies that the k_{obs} value depends on [AMP] hyperbolically and on c_0 proportionally.

The fluorescence time courses at various c_0 and [AMP] were curve-fitted to Eq. 3 to obtain the k_{obs} values. Figure 3B shows the dependence of k_{obs} on [AMP] when $c_0 = 0.1$ μM. As expected, the k_{obs} value depended on [AMP] hyperbolically. The inset of Fig. 3B shows the dependence of k_{obs} on c_0 when [AMP] = 80 μM. Proportionality between k_{obs} and c_0 was also observed when [AMP] = 10 μM and when [AMP] = 800 μM (data not shown). These results agree well with Eq. 6, supporting the validity of Scheme 4. The kinetic parameters were estimated from these data as $k_{+1} = 0.29\ \mu\mathrm{M}^{-1}\cdot\mathrm{s}^{-1}$ and $k_{-1}/k_{+2} = 57\ \mu$M.

The fluorescence change ($Y_\infty - Y_0$) by the reaction was constant over a wide range of [AMP] (20-400 μM) when c_0 was constant, indicating that the binding of α, β, and AMP is tight enough under the conditions of these experiments. This result justifies the simplification of Scheme 4, where the dissociation of AMP from α-β-AMP is omitted. The dissociation of α-β-AMP will be described later.

Isomerization and FAD Binding of α-β-AMP—We previously (*15*) demonstrated that α-β-AMP exists in an equilibrium between two different forms (A and A*) and only one of them (A) combines with FAD to become the holoprotein.

$$\mathrm{A}^{*} \underset{k_{-3}}{\overset{k_{+3}}{\rightleftharpoons}} \mathrm{A},\ \mathrm{A}+\mathrm{FAD} \underset{k_{-4}}{\overset{k_{+4}}{\rightleftharpoons}} \text{holoprotein} \qquad (7)$$

The time course of the reaction between α-β-AMP and an excess of FAD obeys a double exponential function of time. The observed rate constants of the first and second phases

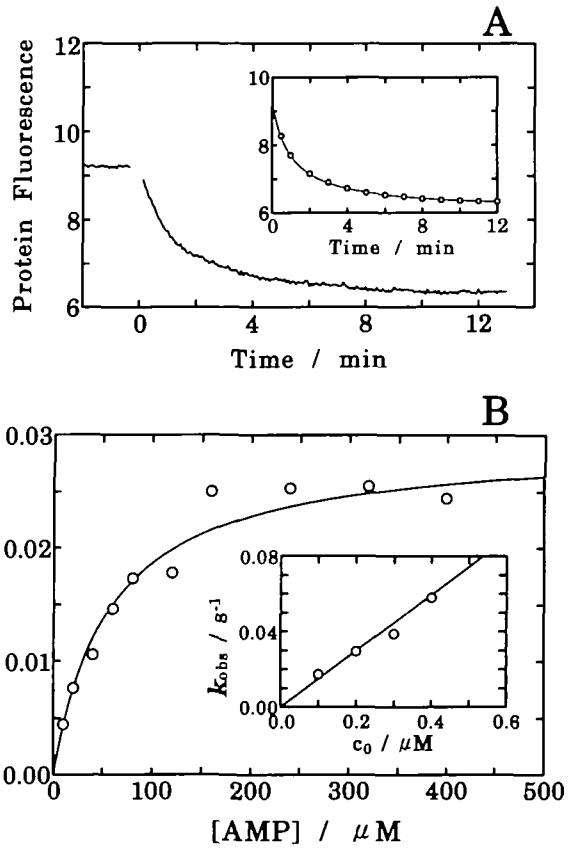

Fig. 3. **A: Protein fluorescence time course of the binding of α, β, and AMP.** Before the reaction, urea-denatured α and β were diluted with the buffer solution to give final concentrations of 0.1 μM in 2 ml. At zero time, 4 μl of solution of AMP was added to the solution of the refolded subunits to give the final concentration of 80 μM. **Inset: The circles show the data of fluorescence value at several points.** The best- fit curve for the function $Y(t) = (Y_0 - Y_\infty)/(k_{\mathrm{obs}}t+1) + Y_\infty$ is shown. **B: Dependence of k_{obs} on AMP concentration.** The concentrations of α and β were both 0.1 μM. The best-fit curve was drawn according to the equation $k_{\mathrm{obs}} = a[\mathrm{AMP}]/(b+[\mathrm{AMP}])$, with the parameters $a = 0.0293\ \mathrm{s}^{-1}$ and $b = 57.1\ \mu$M. **Inset: Dependence of k_{obs} on subunit concentration.** The concentration of AMP was 80 μM. The concentrations (c_0) of α and β were set to be identical to each other.

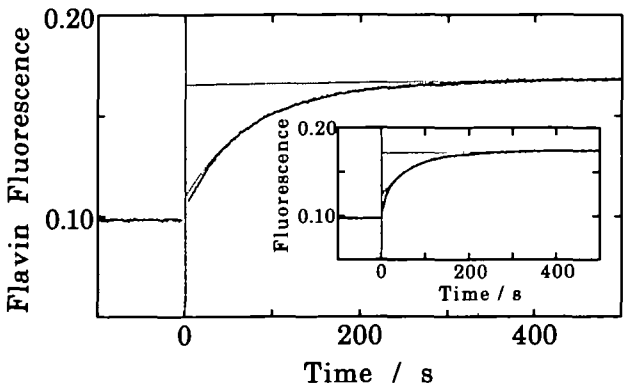

Fig. 4. **Time course of the binding between FAD and α-β-AMP.** At zero time, 2 μl of stock solution of α-β-AMP (60 μM) was added to the 2-ml solution of FAD. The conditions after the mixing were 0.4 μM FAD and 0.06 μM α-β-AMP. In the main panel, the buffer conditions both for the stock solution of α-β-AMP and for the reaction with FAD were as described in "MATERIALS AND METHODS" (5% v/v glycerol). In the inset, the stock solution contained 15% v/v glycerol, while the conditions of the reaction mixture was the same as the main panel (5% v/v glycerol). The dotted curves show the reaction phases separated by curve-fitting: the data of the main panel after 50 s were fitted to $Y(t) = a_2\exp(-k_2t) + a_3t + a_4$ and the data of the inset after 0 s were fitted to $Y(t) = a_1\exp(-k_1t) + a_2\exp(-k_2t) + a_3t + a_4$.

Downloaded from http://jb.oxfordjournals.org/ at Changhua Christian Hospital on October 2, 2012

(k_1 and k_2, respectively) are represented as follows (*15*).

$$k_1=\frac{1}{2}\{k_{+3}+k_{-3}+k_{+4}[\mathrm{FAD}]+k_{-4} +[(k_{+3}+k_{-3}+k_{+4}[\mathrm{FAD}]+k_{-4})^2 -4(k_{+3}k_{+4}[\mathrm{FAD}]+k_{+3}k_{-4}+k_{-3}k_{-4})]^{1/2}\} \quad (8)$$

$$k_2=\frac{1}{2}\{k_{+3}+k_{-3}+k_{+4}[\mathrm{FAD}]+k_{-4} -[(k_{+3}+k_{-3}+k_{+4}[\mathrm{FAD}]+k_{-4})^2 -4(k_{+3}k_{+4}[\mathrm{FAD}]+k_{+3}k_{-4}+k_{-3}k_{-4})]^{1/2}\} \quad (9)$$

α-β-AMP can be prepared in two different ways: by mixing α, β, and AMP (as described above) and by releasing the FAD from the holoprotein (*20*). These two kinds of α-β-AMP showed the same FAD-binding time course under the same conditions (data not shown), confirming the identity between them. In the experiments described below, we used α-β-AMP prepared by detaching the FAD from the holoprotein, because of the simplicity of this method.

We previously (*15*) determined the values of k_{+3}, k_{-3}, k_{+4}, and k_{-4} under conditions different from those of this study. Some modifications of the procedure were needed to determine the kinetic parameters in this study. Figure 4 (main panel) shows the time course of the reaction between α-β-AMP and an excess of FAD: the amplitude of the first phase was too small to detect clearly. According to Scheme 7, the two phases are roughly explained as follows (*15*). The fast phase corresponds to the diminishing of A by binding with FAD, and the slow phase corresponds to the slow conversion of A* to A. Thus, the amplitude of the fast phase is expected to be enlarged when the [A]/[A*] ratio at the start of the reaction is raised. We previously reported that the A* $\rightleftarrows$ A equilibrium is shifted rightward by anions or glycerol (*20*). In the experiment in the inset of Fig. 4, α-β-AMP was preincubated in a high concentration of glycerol (15% v/v) but the reaction mixture contained 5% v/v glycerol [in the main panel, the glycerol concentration was 5%v/v both for the preincubation and for the reaction with FAD]. As expected, the fast phase became obvious after preincubation with the high concentration of glycerol. We could measure both the phases of the reaction by this method.

The time courses fitted better with a modified function $Y(t)=a_1\exp(-k_1t)+a_2\exp(-k_2t)+a_3t+a_4$ than the simple double exponential function $Y(t)=a_1\exp(-k_1t)+a_2\exp(-k_2t)+a_4$. The requirement of the term a_3t arises from the very slow fluorescence enhancement after the completion of the second phase. This is due to the slow re-association of the small amounts of α and β which had dissociated in the stock solution of α-β-AMP (mentioned later).

Figure 5, A and B, shows the k_1 and k_2 values obtained by curve-fitting of the time courses at various FAD concentrations. These k_1 and k_2 data sets were simultaneously curve-fitted to Eqs. 8 and 9, respectively, to obtain the four kinetic parameters. They were estimated as $k_{+3}=(2.48\pm0.12)\times10^{-2}\ \mathrm{s}^{-1}$, $k_{-3}=(3.70\pm0.35)\times10^{-2}\ \mathrm{s}^{-1}$, $k_{+4}=0.154\pm0.010\ \mu\mathrm{M}^{-1}\cdot\mathrm{s}^{-1}$, and $k_{-4}=(0.98\pm0.80)\times10^{-3}\ \mathrm{s}^{-1}$ [(best-fit value) $\pm$ (standard deviation)]. The estimation of the k_{-4} value is relatively unreliable because the standard deviation is similar to the best-fit value. The k_{-4} value will be estimated more carefully in a later section.

Which of A and A Is Formed First by the Binding of α, β, and AMP?* —If A is the first product, the reaction is expressed as

$$\alpha+\beta+\mathrm{AMP}\longrightarrow \mathrm{A}\underset{k_{-3}}{\overset{k_{+3}}{\rightleftharpoons}}\mathrm{A}^*,\ \mathrm{A}+\mathrm{FAD}\underset{k_{-4}}{\overset{k_{+4}}{\rightleftharpoons}}\text{holoprotein} \quad (10)$$

Conversely, if A* is formed earlier, the reaction is expressed as

$$\alpha+\beta+\mathrm{AMP}\longrightarrow \mathrm{A}^*\underset{k_{-3}}{\overset{k_{+3}}{\rightleftharpoons}}\mathrm{A},\ \mathrm{A}+\mathrm{FAD}\underset{k_{-4}}{\overset{k_{+4}}{\rightleftharpoons}}\text{holoprotein} \quad (11)$$

The association of α, β, and AMP (the first step of Schemes 10 and 11) obeys Eq. 5. The other kinetic parameters were determined in the preceding section. Figure 6A shows the simulated holoprotein concentration time courses. Based on Scheme 10 (curve **a**), the first product (A) can combine with FAD instantly, so that the production of the holoprotein is initiated immediately after the start of the reaction. On the other hand, based on Scheme 11 (curve **b**), the first product (A*) cannot associate with FAD until it converts to A, so that the time course of holoprotein shows a clear lag phase.

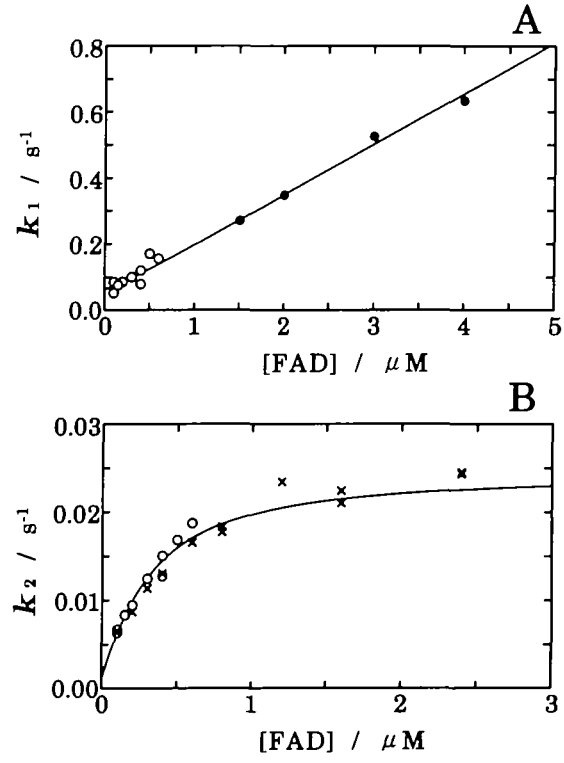

Fig. 5. **Dependence on FAD concentration of k_1 (A) and k_2 (B) of the binding reaction between FAD and α-β-AMP.** The observed rate constants of the fast and slow phases (k_1 and k_2, respectively) were determined by curve-fitting of the time course, as described in the legend to Fig. 4. The data of symbol '×' were obtained by the experiments where α-β-AMP was preincubated in the same buffer as used in the binding reaction. The data of symbol 'O' were obtained by the experiments where α-β-AMP was preincubated with 15% v/v glycerol to enhance the amplitude of the fast phase. The data of the symbol '●' were also obtained with the preincubation with 15% v/v glycerol but by using a stopped-flow apparatus. The glycerol concentration for the binding reactions was 5% v/v for all the data. The best-fit curves obtained with Eqs. 8 and 9 are shown.

Downloaded from http://jb.oxfordjournals.org/ at Changhua Christian Hospital on October 2, 2012

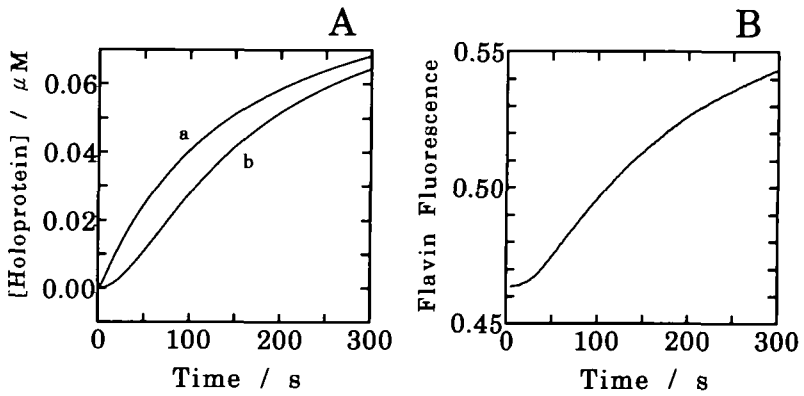

Fig. 6. **A: Simulated time course of holoprotein concentration after mixing α, β, AMP, and FAD.** The reaction of 0.1 μM α and β, 20 μM AMP, and 2 μM FAD was simulated according to Scheme 10 (curve a) or Scheme 11 (curve b). **B: Flavin fluorescence time course of the reaction of α, β, AMP, and FAD.** Before the reaction, urea-denatured α and β were allowed to refold. At zero time, FAD and AMP were added. The conditions of the reaction were 0.1 μM α and β, 20 μM AMP, and 2 μM FAD.

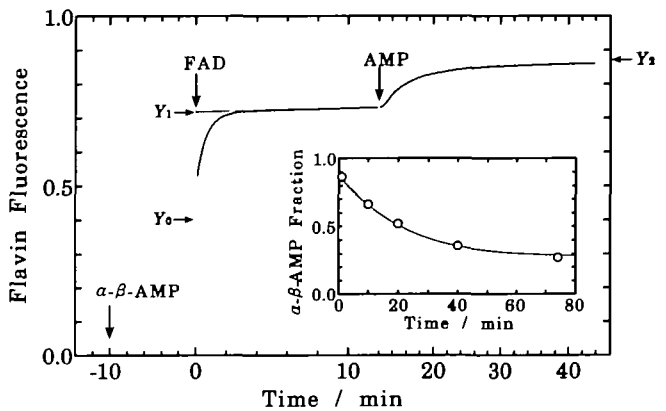

Fig. 7. **Time course of the reaction for investigating the dissociation of α-β-AMP.** The α-β-AMP was stocked in the same buffer as that for the reaction. At -10 min, 10 μl of α-β-AMP (52 μM) was mixed with 1,990 μl of buffer solution in the spectrophotometric cell to give the final concentration of 0.26 μM. At 0 min, 5 μl of FAD solution was added to the reaction mixture to give the final concentration of 2 μM. At 12 min, 5 μl of AMP solution was added to the reaction mixture to give the final concentration of 20 μM. The arrow Y_0 indicates the fluorescence value of 2 μM FAD without α-β-AMP. The Y_1 value is the linearly extrapolated value from the time course at 4-12 min to zero time. The Y_2 value is the final fluorescence. **Inset: Decay of fraction of α-β-AMP after the dilution.** The experiments similar to that in the main panel were carried out with various preincubation times (the time from the dilution of α-β-AMP to the addition of FAD). The values of $(Y_1-Y_0)/(Y_2-Y_0)$ were plotted against the preincubation time. The curve shows the simulated time course according to Scheme 12 with $k_{-2}=8\times10^{-4}$ s^{-1}.

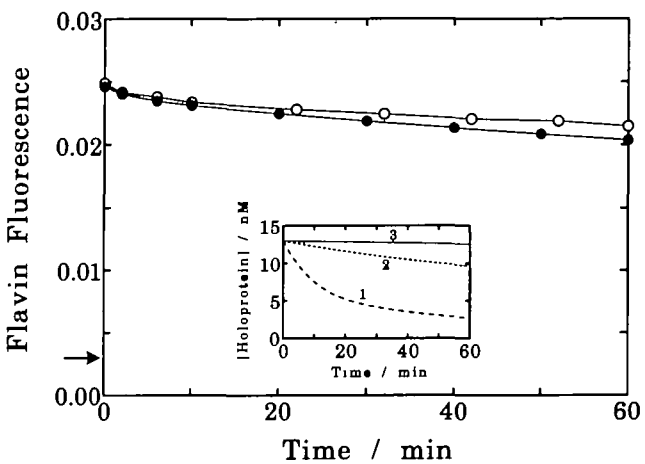

Fig. 8. **Flavin fluorescence time course after the dilution of holoprotein.** The holoprotein was diluted from 26 μM to 13 nM in the buffer solution containing 0 (●) or 1 μM (○) FAD. The arrow indicates the fluorescence intensity of 13 nM free FAD. **Inset: Simulated time course of the reaction after the dilution of holoprotein to 13 nM in the absence of FAD.** The reaction was simulated according to Scheme 1. The k_{-4} value was set at 10^{-3} (1), 10^{-4} (2), or 10^{-5} s^{-1}(3).

The experimentally measured time course (Fig. 6B), showing a clear lag phase, was quite similar to curve **b** in Fig. 6A. This result indicates that Scheme 11 holds true.

Dissociation Rate of AMP from α-β-AMP—The dissociation of α, β, and AMP was observed by diluting the solution of α-β-AMP. In the experiment shown in Fig. 7, the stock solution of α-β-AMP (52 μM) was diluted to 0.26 μM at -10 min. After 10-min preincubation, 2 μM FAD was added to the diluted α-β-AMP. Although the reaction between FAD and α-β-AMP is biphasic, only the second phase was detected clearly because of the rapidity of the first phase (relaxation time is 5.1 s). After the completion of the second phase, the flavin fluorescence continued to increase very slowly (4-12 min), reflecting the association of FAD with α and β subunits which had split from α-β-AMP during the preincubation (-10-0 min). The slow fluorescence enhancement (4-12 min) was made fast after the addition of 20 μM AMP (12 min), confirming that the slow fluorescence enhancement was due to the re-association of the split subunits.

The arrow Y_0 in Fig. 7 indicates the fluorescence value of 2 μM free FAD. The Y_1 value was obtained by linear extrapolation from the time course at 4-12 min to zero time. The difference between Y_1 and Y_0 corresponds to the sum of the concentrations of A* and A at zero time. The Y_2 value indicates the final fluorescence value. The difference between Y_2 and Y_0 corresponds to the total concentration of the protein. Thus the ratio $r=(Y_1-Y_0)/(Y_2-Y_0)$ indicates the proportion of α-β-AMP at zero time to the total protein. The r values obtained with various preincubation times are shown in the inset of Fig. 7. The dissociation of α-β-AMP after the dilution can be simulated according to the following scheme.

$$A \underset{k_{-3}}{\overset{k_3}{\rightleftharpoons}} A^* \underset{k_{-2}}{\overset{k_{-2}}{\rightleftharpoons}} AMP+\alpha\text{-}\beta^A,\ \alpha\text{-}\beta^A \underset{k_{-1}}{\overset{k_{-1}}{\rightleftharpoons}} \alpha+\beta \qquad (12)$$

All the parameters in this scheme were estimated above,

Downloaded from http://jb.oxfordjournals.org/ at Changhua Christian Hospital on October 2, 2012

except for the k_{-2} value and the k_{-1}/k_{+1} ratio. The simulation was repetitively tried with different k_{-2} values. The best-fit curve was obtained when $k_{-2}=8.0\times10^{-4}$ s^{-1}. The same k_{-2} value was also obtained at a lower concentration (0.075 μM) of α-β-AMP. The uncertainty of the dissociation constant ($K_{d1}=k_{-1}/k_{+1}$) of α-β^{A} caused no serious error: the simulated time courses with $K_{d1}=1$ μM and $K_{d1}=100$ μM (not shown) were almost the same as that obtained with $K_{d1}=10$ μM (shown in the inset).

Dissociation Rate of FAD from Holoprotein—The dissociation of FAD from holoprotein after dilution should proceed by the reactions of Scheme 1 leftward. The inset in Fig. 8 shows the simulation of the dissociation of 13 nM holoprotein. The k_{-4} value was set to be 10^{-3}(curve **1**), 10^{-4} (**2**), and 10^{-5} s^{-1}(**3**).

The closed circles in Fig. 8 show the experimentally obtained time course of flavin fluorescence after the dilution of the holoprotein from 26 μM to 13 nM. The arrow in Fig. 8 indicates the fluorescence intensity of 13 nM free FAD: if all the bound FAD in the holoprotein is detached, the fluorescence intensity should be quenched to this level. About 20% release of FAD in 1 h (closed circles) corresponds to $k_{-4}=10^{-4}$ s^{-1} (curve **2** in the inset). If this k_{-4} value is correct, only 0.4% of the bound FAD should be released in the presence of 1 μM free FAD, according to the simulation (not shown). However, in reality, about 15% of the FAD was released in 1 h even in the presence of 1 μM FAD (open circles). This can be explained by a side reaction, such as irreversible degeneration of the holoprotein. The FAD dissociation by k_{-4} is very small even in the absence of 1 μM FAD (closed circles). Therefore, the k_{-4} value is estimated to be smaller than 10^{-4}s^{-1}. The FAD release due to Scheme 2 can be ignored because the AMP release from the holoprotein is very slow ($k_{-7}<10^{-5}$s^{-1}, described later).

Binding of α, β, and FAD—When α, β, and FAD were mixed, very slow formation of α-β-FAD was observed (Fig. 1, curve **1**). In the previous sections, it was demonstrated that α and β subunits weakly interact with each other and that a single subunit does not associate with FAD. Therefore we can consider the binding mechanism of α, β, FAD to be as follows.

$$\alpha+\beta \underset{k_{-5}}{\overset{k_{+5}}{\rightleftharpoons}} \alpha\text{-}\beta^{F},\ \alpha\text{-}\beta^{F}+\mathrm{FAD} \underset{k_{-6}}{\overset{k_{+6}}{\rightleftharpoons}} \alpha\text{-}\beta\text{-FAD} \qquad (13)$$

Here, α-β^{F} is the heterodimer form which associates with FAD. Using the steady state method, the reaction velocity ($v=\mathrm{d}[\alpha\text{-}\beta\text{-FAD}]/\mathrm{d}t$) is represented as

$$v=\frac{k_{+5}[\mathrm{FAD}][\alpha][\beta]}{k_{-5}/k_{+6}+[\mathrm{FAD}]}, \qquad (14)$$

when the dissociation rate of α-β-FAD is negligible.

Figure 9 shows the experimentally obtained initial v values at $[\alpha]=[\beta]=0.2$ μM and at various points of [FAD]. The hyperbolic dependence of v on [FAD] is consistent with Eq. 14. The inset of Fig. 9 shows the dependence of v on $[\alpha][\beta]$ when $[\mathrm{FAD}]=0.5$ μM. Proportionality between v and $[\alpha][\beta]$ was also observed when $[\mathrm{FAD}]=0.1$ μM and when $[\mathrm{FAD}]=2$ μM (data not shown). These results agree well with Eq. 14, supporting the validity of Scheme 13. The kinetic parameters were estimated from these data as $k_{+5}=7.2\times10^{-4}$ μM^{-1}·s^{-1} and $k_{-5}/k_{+6}=0.78$ μM. It should be noted that the α-β^{F} form in Scheme 13 is distinct from the α-β^{A} form in Scheme 4 because the association rate constants from monomeric α and β are largely different between them. The k_{-6} value was estimated to be smaller than 10^{-4} s^{-1} from similar experiments to those carried out for the estimation of the k_{-4} value (Fig. 8).

Binding of AMP with α-β-FAD—The isoelectric points of the holoprotein and α-β-FAD are 6.7 and 7.1, respectively (*6*). Using this difference, the binding of AMP with α-β-FAD was investigated (see the legend to Fig. 10).

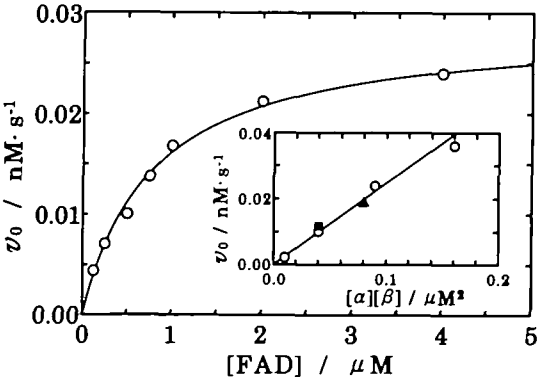

Fig. 9. **The initial rate of FAD binding with 0.2 μM α and β at various FAD concentrations.** The initial FAD binding rate ($v_0=(\mathrm{d}[\alpha\text{-}\beta\text{-FAD}]/\mathrm{d}t)_{t=0}$) was determined from the slope of the flavin fluorescence time course in the initial few minutes, according to the difference of flavin fluorescence intensity between α-β-FAD and free FAD of known concentration. The best-fit curve was drawn according to the equation $v_0=a[\mathrm{FAD}]/(b+[\mathrm{FAD}])$, where $a=2.9\times10^{-2}$ nM^{-1}·s^{-1} and $b=0.78$ μM. **Inset: The binding rate of 0.5 μM FAD with various concentrations of subunits.** The concentrations of the two subunits were identical to each other in the reactions of symbol '○.' The concentrations of α and β were respectively 0.1 and 0.4 μM for '■' and 0.4 and 0.2 μM for '▲.'

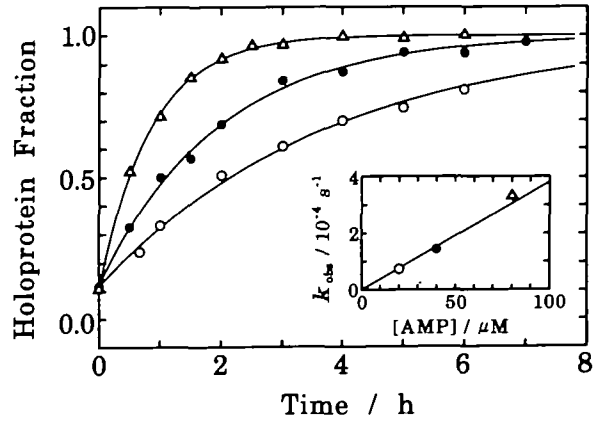

Fig. 10. **Time course of the binding between AMP and α-β-FAD.** The α-β-FAD was prepared as described previously (*6*). α-β-FAD (5 μM) was incubated with 20 (○), 40 (●), or 80 μM (△) AMP. After the intended incubation time, 10 μl of the reaction mixture was applied to isoelectric focusing for separating the holoprotein and α-β-FAD. The two bands visualized by staining were measured by a densitometer and the holoprotein fraction was calculated by $r=H/(H+F)$, where H and F are the planimetrically determined holoprotein and α-β-FAD, respectively. The main panel shows the r value as a function of the incubation time. The data of each time course was curve-fitted to $r=a\exp(-k_{obs}t)+b$, and the obtained k_{obs} values are plotted against the AMP concentration in the inset.

Downloaded from http://jb.oxfordjournals.org/ at Changhua Christian Hospital on October 2, 2012

Figure 10 shows the time courses of the binding of α-β-FAD with different concentrations of AMP, under the conditions where the concentration of AMP is much higher than α-β-FAD. The data set of each time course fitted well with a single exponential function, and the observed rate constant was proportional to the AMP concentration as shown in the inset of Fig. 10. These results can be explained by a simple bimolecular reaction model.

$$\alpha\text{-}\beta\text{-FAD}+\text{AMP} \underset{k_{-7}}{\overset{k_{+7}}{\rightleftharpoons}} \text{holoprotein}$$

The kinetic parameters were estimated as $k_{+7}=3.8\times10^{-6}$ $\mu M^{-1}\cdot s^{-1}$ and $k_{-7}<10^{-5}$ s^{-1}. The binding experiment under conditions where the concentration of α-β-FAD is much higher than AMP gave essentially the same k_{+7} and k_{-7} values, supporting the validity of this scheme. Until now, we have observed only one form of α-β-FAD, unlike α-β-AMP.

DISCUSSION

Overview of the Assembly—In this study, we clarified that the holoprotein of ETF can be formed by the two different pathways (Schemes 1 and 2). The values of the kinetic parameters in the schemes are summarized in Table I.

The interaction between α and β is so weak that most molecules are in the monomer states under the conditions employed in this study (0.1-0.5 μM subunits). The binding rate of $\alpha+\beta+$AMP (curve **1** in Fig. 11) is much higher than that of $\alpha+\beta+$FAD (the curve in the main panel of Fig. 9) [the concentrations of α and β are the same in both figures]. The maximum binding rate of AMP is about 400 times higher than that of FAD. The resulting α-β-AMP associates with FAD much more rapidly than $\alpha+\beta$ does (see the next section). Therefore, the main pathway of the holoprotein formation is Scheme 1. As shown in Fig. 11, the reaction of α-β-FAD+AMP (curve **2**) is much slower than $\alpha+\beta+$AMP (curve **1**). The binding of AMP with the protein is prevented by the previous FAD binding.

TABLE I. **Kinetic parameters of the reactions included in the assembly pathway of ETF.**

$k_{+1}=0.29\ \mu M^{-1}\cdot s^{-1}$
$K_{d1}=k_{-1}/k_{+1}>1\ \mu M$
$k_{-1}=k_{+1}\ K_{d1}>0.29\ s^{-1}$
$k_{+2}=k_{-1}/(57\ \mu M)>5\times10^{-3}\ \mu M^{-1}\cdot s^{-1}$
$k_{-2}=8.0\times10^{-4}\ s^{-1}$
$k_{+3}=2.5\times10^{-2}\ s^{-1}$
$k_{-3}=3.7\times10^{-2}\ s^{-1}$
$k_{+4}=0.15\ \mu M^{-1}\cdot s^{-1}$
$k_{-4}<10^{-4}\ s^{-1}$
$k_{+5}=7.2\times10^{-4}\ \mu M^{-1}\cdot s^{-1}$
$K_{d5}=k_{-5}/k_{+5}>1\ \mu M$
$k_{-5}=k_{+5}K_{d5}>7.2\times10^{-4}\ s^{-1}$
$k_{+6}=k_{-5}/(0.78\ \mu M)>9.2\times10^{-4}\ \mu M^{-1}\cdot s^{-1}$
$k_{-6}<10^{-4}\ s^{-1}$
$k_{+7}=3.8\times10^{-6}\ \mu M^{-1}\cdot s^{-1}$
$k_{-7}<10^{-5}\ s^{-1}$

The assembly pathways are as follows:

$$\alpha+\beta \underset{k_{-1}}{\overset{k_{+1}}{\rightleftharpoons}} \alpha\text{-}\beta^{A} \underset{k_{-2}}{\overset{k_{+2}[AMP]}{\rightleftharpoons}} A^{*} \underset{k_{-3}}{\overset{k_{+3}}{\rightleftharpoons}} A \underset{k_{-4}}{\overset{k_{+4}[FAD]}{\rightleftharpoons}} \text{holoprotein}$$

$$\alpha+\beta \underset{k_{-5}}{\overset{k_{+5}}{\rightleftharpoons}} \alpha\text{-}\beta^{F} \underset{k_{-6}}{\overset{k_{+6}[FAD]}{\rightleftharpoons}} \alpha\text{-}\beta\text{-FAD} \underset{k_{-7}}{\overset{k_{+7}[AMP]}{\rightleftharpoons}} \text{holoprotein}$$

α-β^{A} and α-β^{F} are two different forms of the α-β complex and A* and A are two different forms of the α-β-AMP complex.

Effect of AMP on the Assembly—The experiment of Fig. 1 clearly shows that the binding between FAD and the subunits is promoted by AMP. The function of AMP can be quantitatively discussed by comparing the FAD binding rate between $\alpha+\beta$ and α-β-AMP. According to Eq. 14 with the assumption that the backward dissociation is negligible, the time course of the reaction $\alpha+\beta+$FAD should be a hyperbolic function of time when $[\alpha]=[\beta]$. The time (τ_1) required for the half completion of $\alpha+\beta+$FAD is given by

$$\tau_1=\frac{1}{k_{+5}c}=\frac{1{,}400\ \mu M\cdot s}{c}, \qquad (15)$$

when $[\alpha]=[\beta]=c$ and [FAD] is infinite. On the other hand, the binding of α-β-AMP+FAD obeys a double exponential function of time as shown in Fig. 4. The greater part of the fluorescence increment in Fig. 4 belongs to the slow phase. Thus the rate of the reaction can be simply characterized by the half-completion time (τ_2) of the slow phase as follows at infinite FAD concentration.

$$\tau_2=\frac{\ln 2}{k_{+3}}=28\ s$$

Under the conditions employed in this study (0.1-0.5 μM subunits), the FAD binding is much faster with α-β-AMP ($\tau_2=28$ s) than with $\alpha+\beta$ ($\tau_1=2{,}800$-$14{,}000$ s).

The binding rate of $\alpha+\beta+$FAD is dependent on the subunit concentration. According to Eq. 15, the subunits have to be concentrated to more than 50 μM to show the similar FAD binding rate of α-β-AMP. However, it is difficult to attain this situation because the subunits are susceptible to irreversible denaturation or aggregation at such a high concentration (*11*). The subunits of oligomeric proteins present hydrophobic surfaces, which is important for subunit-subunit contact in the oligomeric forms. The aggregation is probably due to the non-specific interactions between the hydrophobic surfaces of the subunits. The aggregation is observed in the concentrated solutions of α, β, or the mixture of both, but not observed for the ligand-

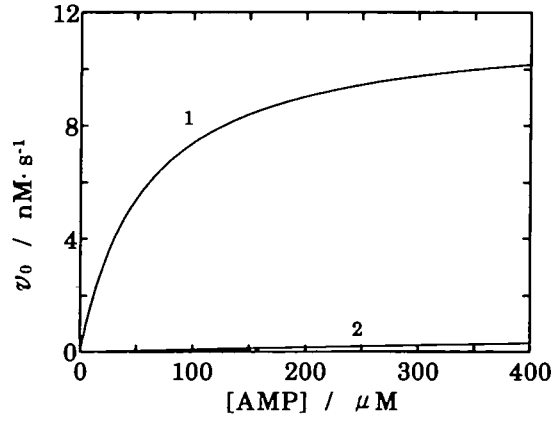

Fig. 11 **Calculated initial binding rates of reactions, $\alpha+\beta+$AMP (curve 1) and α-β-FAD+AMP (curve 2), as a function of the AMP concentration.** The protein concentrations are 0.2 μM α and β (1) and 0.2 μM α-β-FAD (2). The initial binding rates (v_0) of curve 1 were calculated by using Eq. 5 and those of curve 2 were calculated by $v_0=k_{+7}[\alpha\text{-}\beta\text{-FAD}][AMP]$.

Downloaded from http://jb.oxfordjournals.org/ at Changhua Christian Hospital on October 2, 2012

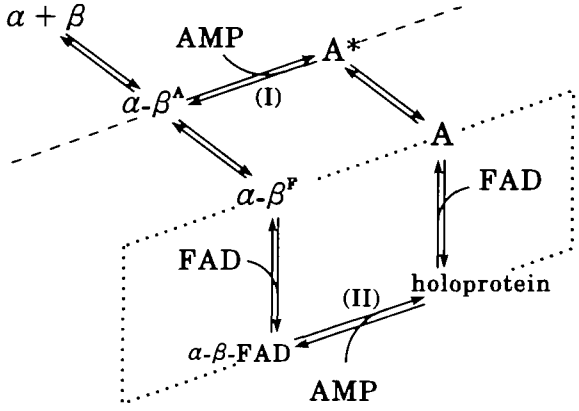

Fig. 12. **Assembly pathway of ETF**. The dashed line links loose conformations and the dotted line links compact conformations.

binding dimeric forms (α-β-AMP, α-β-FAD, and α-β-FAD-AMP)(*11*).

The dependence of the binding rate of $\alpha+\beta$+FAD on the subunit concentration is due to the weak binding between α and β. As the subunit concentration increases, the proportion of α-β^F is raised and subsequently the FAD binding is enhanced. The binding of AMP with $\alpha+\beta$ induces the dimerization of the subunits and results in the increase of the concentration of A. By this mechanism, AMP promotes the binding between FAD and the apoprotein even in low subunit concentrations.

Two Conformations of Heterodimer—We previously (*20*) reported the structural difference between the two forms of α-β-AMP (A* and A). The A form is compactly folded while the A* form is partially unfolded. The circular dichroism at 220 nm of A* is about 75% of that of A, indicating that A has more structured peptide backbone than A*. In addition, A* and A show very different molecular weights [120,000 (A*) and 56,000(A)] on gel filtration. These values correspond to Stokes radii of 42 (A*) and 32 Å (A) (*21*). [The true molecular weights have been confirmed by light-scattering method to be about 60,000 for both A* and A.] The conformations of the holoprotein (*20*) and α-β-FAD (*6*) are similar to the A form with respect to the retention time on gel filtration and the far-UV circular dichroism spectrum. This finding seems reasonable because FAD is bound with the A form not with the A* form: the compact conformation has the proper FAD-binding site while the loose conformation does not.

The rate constant of formation of α-β^A from monomeric subunits ($k_{+1}=0.29\ \mu M^{-1}\cdot s^{-1}$) is much larger than that of α-β^F ($k_{+5}=7.2\times10^{-4}\ \mu M^{-1}\cdot s^{-1}$). The dimerization rate constant should be related with the conformation of the heterodimer. It can be speculated that α-β^A has a relatively loose conformation (immediately after the docking of the subunits) while α-β^F has a compact conformation (additionally folded after the docking). This consideration is consistent with the fact that the product of α-β^A+AMP is the loose A* form and the product of α-β^F+FAD is the compact α-β-FAD.

The pathway of the assembly of ETF can be schematized as in Fig. 12. The molecular species of loose conformation are linked by the dashed line and those of compact conformation are linked by the dotted line. The difference in the AMP-binding site between the loose and compact conformations can be speculated by comparing the rates between the reactions I and II in Fig. 12. The AMP binding rate constant is much larger for α-β^A ($k_{+2}>5\times10^{-3}\ \mu M^{-1}\cdot s^{-1}$) than for α-β-FAD ($k_{+7}=3.8\times10^{-6}\ \mu M^{-1}\cdot s^{-1}$) and the AMP dissociation rate constant is much larger for A* ($k_{-2}=8\times10^{-4}\ s^{-1}$) than for the holoprotein ($k_{-7}<10^{-5}\ s^{-1}$). Thus both association and dissociation of AMP are much faster for the looser conformation. This result leads to a speculation that the AMP-binding site is exposed to the solvent in the loose conformation, while it is buried in the protein in the compact conformation.

As a result, the loose conformation is suitable for AMP binding while the compact conformation is suitable for FAD binding.

REFERENCES

1. Crane, F.L. and Beinert, H. (1956) On the mechanism of dehydrogenation of fatty acyl derivatives of coenzyme A: II. The electron-transferring flavoprotein. *J. Biol. Chem.* **218**, 717-731
2. Crane, F.L., Mii, S., Hauge, J.G., Green, D.E., and Beinert, H. (1956) On the mechanism of dehydrogenation of fatty acyl derivatives of coenzyme A: I. The general fatty acyl coenzyme A dehydrogenase. *J. Biol. Chem.* **218**, 701-716
3. Noda, C., Rhead, W.J., and Tanaka, K. (1980) Isovaleryl-CoA dehydrogenase: Demonstration in rat liver mitochondria by ion exchange chromatography and isoelectric focusing. *Proc. Natl. Acad. Sci. USA* **77**, 2646-2650
4. Ikeda, Y., Dabrowski, C., and Tanaka, K. (1983) Separation and properties of five distinct acyl-CoA dehydrogenases from rat liver mitochondria. *J. Biol. Chem.* **258**, 1066-1067
5. Ruzicka, F.J. and Beinert, H. (1977) A new iron-sulfur flavoprotein of the respiratory chain: A component of the fatty acid β oxidation pathway. *J. Biol. Chem.* **252**, 8440-8445
6. Sato, K., Nishina, Y., and Shiga, K. (1993) Electron-transferring flavoprotein has an AMP-binding site in addition to the FAD-binding site. *J. Biochem.* **114**, 215-222
7. DuPlessis, E.R., Rohlfs, R.J., Hille, R., and Thorpe, C. (1994) Electron-transferring flavoprotein from pig and the methylotrophic bacterium W3A1 contains AMP as well as FAD. *Biochem. Mol. Biol. Int.* **32**, 195-199
8. Furuta, S., Miyazawa, S., and Hashimoto, T. (1981) Purification and properties of rat liver acyl-CoA dehydrogenases and electron transfer flavoprotein. *J. Biochem.* **90**, 1739-1750
9. Gorelick, R.J., Mizzer, J.P., and Thorpe, C. (1982) Purification and properties of electron-transferring flavoprotein from pig kidney. *Biochemistry* **21**, 6936-6942
10. McKean, M.C., Beckmann, J.D., and Frerman F.E. (1983) Subunit structure of electron transfer flavoprotein. *J. Biol. Chem.* **258**, 1866-1870
11. Sato, K., Nishina, Y., and Shiga, K. (1994) Preparation of separated α and β subunits of electron-transferring flavoprotein in unfolded forms and their restoration to the native holoprotein form. *J. Biochem.* **116**, 147-155
12. White, S.A., Mathews, F.S., Rohlfs, R.J., and Hille, R. (1994) Crystallization and preliminary crystallographic investigation of electron-transfer flavoprotein from the bacterium *Methylophilus* W3A1. *J. Mol. Biol.* **240**, 265-266
13. Roberts, D.L., Herrick, K.R., Frerman, F.E., and Kim, J.-J.P. (1995) Crystallization and preliminary X-ray analysis of electron transfer flavoproteins from human and *Paracoccus denitrificans*. *Protein Sci.* **4**, 1654-1657
14. Sato, K., Nishina, Y., and Shiga, K. (1996) *In vitro* refolding and unfolding of subunits of electron-transferring flavoprotein: Characterization of the folding intermediates and the effects of FAD and AMP on the folding reaction. *J. Biochem.* **120**, 276-285
15. Sato, K., Nishina, Y., Shiga, K., Tojo, H., and Tada, M. (1991) The existence of two different forms of apo-electron-transferring

Downloaded from http://jb.oxfordjournals.org/ at Changhua Christian Hospital on October 2, 2012

flavoprotein. *J. Biochem.* **109**, 734-740
16. Walsh, C., Fisher, J., Spencer, R., Graham, D.W., Ashton, W.T., Brown, J.E., Brown, R.D., and Rogers, E.F. (1978) Chemical and enzymatic properties of riboflavin analogues. *Biochemistry* **17**, 1942-1951
17. Bock, R.M., Ling, N.-S., Morell, S.A., and Lipton, S.H. (1956) Ultraviolet absorption spectra of adenosine-5′-triphosphate and related 5′-ribonucleotides. *Arch. Biochem. Biophys.* **62**, 253-264
18. Hayashi, Y., Matsui, H., and Takagi, T. (1989) Membrane protein molecular weight determined by low-angel laser light-scattering method coupled with high-performance gel chromatography. *Methods Enzymol.* **172**, 514-528
19. Takagi, T. (1990) Application of low-angle laser light scattering detection in the field of biochemistry. *J. Chromatogr.* **506**, 409-416
20. Sato, K., Nishina, Y., and Shiga, K. (1992) Anion-induced conformational change of apo-electron-transferring flavoprotein. *J. Biochem.* **111**, 359-365
21. Uversky, V.N. (1993) Use of fast protein size-exclusion liquid chromatography to study the unfolding of proteins which denature through the molten globule. *Biochemistry* **32**, 13288-13298

Downloaded from http://jb.oxfordjournals.org/ at Changhua Christian Hospital on October 2, 2012